Journal of Maps

ISSN: (Print) 1744-5647 (Online) Journal homepage: https://www.tandfonline.com/loi/tjom20

The composite Sierra Bermeja Pluton (southern Iberian Massif): science, heritage and geoconservation

Jon Errandonea-Martin, Fernando Sarrionandia, Josu Junguitu, Manuel Carracedo-Sánchez, Luis Eguíluz & José Ignacio Gil Ibarguchi

To cite this article: Jon Errandonea-Martin, Fernando Sarrionandia, Josu Junguitu, Manuel Carracedo-Sánchez, Luis Eguíluz & José Ignacio Gil Ibarguchi (2019) The composite Sierra Bermeja Pluton (southern Iberian Massif): science, heritage and geoconservation, Journal of Maps, 15:2, 101-111, DOI: 10.1080/17445647.2018.1548981

To link to this article: https://doi.org/10.1080/17445647.2018.1548981

JOURNAL OF MAPS
2018, VOL. 15, NO. 2, 101–111
https://doi.org/10.1080/17445647.2018.1548981

Science

OPEN ACCESS Check for updates

The composite Sierra Bermeja Pluton (southern Iberian Massif): science, heritage and geoconservation

Jon Errandonea-Martin [a], Fernando Sarrionandia[b,c], Josu Junguitu[b,c], Manuel Carracedo-Sánchez[a], Luis Eguíluz[b,c] and José Ignacio Gil Ibarguchi[a]

[a]Department of Mineralogy and Petrology, Faculty of Science and Technology, University of the Basque Country UPV/EHU, Leioa, Spain; [b]Department of Geodynamics, Faculty of Pharmacy, University of the Basque Country UPV/EHU Vitoria-Gasteiz, Spain; [c]General Cartography and Geographic Information Systems Service (SGIKER), Lascaray Research Center, University of the Basque Country UPV/EHU Vitoria-Gasteiz, Spain

ABSTRACT

The Sierra Bermeja Pluton (~60 km^2 surface area) exemplifies a type of controversial granites of the Iberian Massif (European Variscan Belt), the cordierite-bearing 'Serie Mixta' (mixed series) monzogranites. The pluton is included almost completely in the Cornalvo Natural Park (Badajoz, Spain), a relevant target area in Roman times. The geological mapping summarised in the presented map at 1:10,000 scale has revealed a complex intrusive assemblage. Three main cordierite-bearing monzogranite types that show local varieties constitute most of the massif. Monzogranite intrusions are younger towards the centre of the pluton and gave rise to outstanding mappable mingling/mixing zones in some areas. A NE–SW trending reduced dyke complex composed by vaugnerite series rocks, lamprophyres, aplites and quartz dykes, completes the lithological assemblage of the pluton. An inventory of Geologic Points of Interest to promote the geological knowledge of this remarkable protected area and its geoconservation is also presented.

ARTICLE HISTORY
Received 12 September 2018
Revised 8 November 2018
Accepted 13 November 2018

KEYWORDS
Granite mapping; cordierite-bearing monzogranite; vaugnerite series rocks; lamprophyre; Iberian Massif; geoconservation

1. Introduction

Precise geological maps constitute the basis of studies such as those applied in resources exploration, civil engineering, environmental geosciences and natural hazards (Lisle, Brabham, & Barnes, 2011). Indeed, their accuracy is decisive to prevent severe economic and/or human losses, and the progress of the scientific knowledge requires as well accurate maps. This is the case of the Igneous Petrology, where detailed mapping of granitic areas is essential. Granitic rocks dominate the upper continental crust and, since the crust records the evolution of the Earth through time, their study provides essential information about major geological processes (Bonin, Azzouni-Sekkal, Bussy, & Ferrag, 1998; Hawkesworth et al., 2010; Rudnick & Gao, 2014). Igneous intrusions often form large adjacent arrays of multiple plutons (batholiths), in many cases up to several thousands of km^2 in surface area (e.g. Strathbogie Batholith in the Lachlan Fold Belt, Sierra Nevada Batholith in the Cordilleran Belt, Gangdese Batholith of Himalaya, Spanish Central System in the Iberian Variscan Belt, etc.), where the study of discrete magma batches is feasible (Pitcher, 1997; Villaseca & Herreros, 2000). In such extensive batholiths, a regional scale mapping could be the best initial approach (e.g. Casini et al., 2015; Martínez Catalán et al., 2007; Porquet et al., 2017). However, as a result of the usual complex assemblage of different magma pulses, detailed maps are mandatory for specific researches (e.g. Cobbing, 2000; Díez Fernández, Martín Parra, & Rubio Pascual, 2017; Díez Fernández, Rubio Pascual, & Martín Parra, 2018, in press; Sarrionandia et al., 2013).

The interest of mapping granitic areas furthermore transcends the purely scientific realms. Granitoids have been highly exploited through History (e.g. Barral I Altet, 1991; Sureda, 1991). In the Egyptian, Greek and Roman Civilisations, granites represented an essential construction material in dams, aqueducts, temples, circuses and other monumental buildings due to their durability (Barral I Altet, 1991; Sureda, 1991; Wilson Jones, 2000). While this use as building or dimension stone still remains, granites are currently prospective targets of maximum interest since modern technologies require granite-related ore deposits for the increasing demand of Rare Earth Elements (REE), precious and critical metals (Chakhmouradian & Zaitsev, 2012; Linnen, Lichtervelde, & Černý, 2012; Sial, Bettencourt, De Campos, & Ferreira, 2011).

Since geology is part of all natural systems, the care for geological heritage is undeniably essential for an

CONTACT Jon Errandonea-Martin jon.errandonea@ehu.eus Department of Mineralogy and Petrology, Faculty of Science and Technology, University of the Basque Country UPV/EHU, Sarriena street N/N, Leioa, Bizkaia 48940, Spain

effective nature conservation (Brilha, 2002). The preservation of geological entities involves the protection of the space where those objects or entities are found (Carreras & Druguet, 2000). In this sense, protected areas such as National Parks or Natural Reserves play an important role, not only in preserving habitats, ecosystems and species, but also safeguarding landscape features and rock exposures (Dingwall, 2000). In terms of geoconservation (Brocx & Semeniuk, 2007), the recognition of Geoparks (UNESCO Earth-Sciences Division) and the Global Geosites Project (International Union of Geological Sciences, IUGS) are valuable frameworks for the governmental management (e.g. Carreras & Druguet, 2000; Wimbledon et al., 2000). According to IUGS procedures, geological map sheets, at least at scale of 1:50,000, are needed in order to display, among others, the location and extent of a Geosite (Wimbledon et al., 2000).

In this contribution we present a detailed geological map at 1:10,000 scale of a composite granitic pluton, the Sierra Bermeja Pluton, which is encompassed in part within a protected area of remarkable natural and historical interest, the Cornalvo Natural Park (Badajoz province of Spain). Despite the relatively small surface area (~60 km^2), the resulting map reveals a complex igneous architecture consequence of several magma intrusions. The purpose of this contribution is twofold. On one hand, the map constitutes the base for specific contributions on the petrogenesis of the Sierra Bermeja Pluton, and since this pluton is representative of the controversial cordierite-bearing granites of the Iberian Massif, it is intended to serve as reference for upcoming mapping of such granites there and elsewhere. The map also includes a thorough inventory of noticeable geological (Geological Point of Interest, GPI; Table 1) and of other nature sites of interest (Main Map) aimed to be taken into account by the Cornalvo Natural Park administration in terms of geoconservation and geological heritage.

2. Geographical and geological setting

The Sierra Bermeja Pluton (731773.6–746353.8; 4322473.8–4331664.5; UTM zone 29N) is located 15 km northeast of the City of Mérida, at the border of Cáceres and Badajoz provinces (Spain). The main accesses to this pluton depart from the villages of Aljucén, Mirandilla and Trujillanos (Figure 1). This area is encompassed within the Guadiana Basin, south of the Sierra de San Pedro and Montánchez Ranges, and immediately north of the Sierra Bermeja Range (Main Map). The climate is temperate with dry and hot summers (Agencia Estatal de Meteorología de España, AEMET & Instituto Português do Mar e da Atmosfera, IPMA, 2011) characterised in the studied area by low humidity (60–65% as average) and rainfall values (450–550 mm per year as average), not very cold winters (hardly ever < 0°C) and specially dry and hot summers, often above 40°C (AEMET, 2012). The landscape is characterised by a sparse forest ('dehesa'; Main Map, G-1) composed by a variety of holm oak and cork oak groves that cover a smooth topography (250–350 m.a.s.l.) sprinkled with formations of large rounded granitic boulders ('berrocal'; Main Map, G-2, G-3, G-4). The drainage system of the mapped area is governed by the Aljucén and Albarregas Rivers. This hydrographic network, defined by a roughly dendritic pattern, includes minor streams (Fresneda, Muelas, San Pablo and Gamo) and the Cornalvo and Muelas major reservoirs (Main Map, G-5).

The granitic massif is almost completely included within the Cornalvo Natural Park (Decree 27/1993, on 24 February 1993; Law 7/2004, on 19 November 2004). Also, since the year 2000 the area is included in the European network Natura 2000 and is regulated as Protected Area for Birds (ZEPA; Directive 79/409/CEE, on 2 April 1989), Places of Community Interest (LIC, Directive 92/43/CEE, on 19 July 2006) and Area of Special Conservation (ZEC, Decree 110/2015, on 19 May 2015). This region has been occupied since the Antiquity, standing out the uncountable Roman remains related to the colony of Emerita Augusta (current Mérida). In fact, the granitic rocks were used by the Romans for the construction of roads and bridges (Camino de la Plata/Vía de la Plata), monumental buildings of Emerita Augusta (e.g. the amphitheatre or the theatre), and structures for water supply such as the Cornalvo and Proserpina Dams or the Los Milagros Aqueduct (Álvarez Martínez & Nogales Basarrarte, 2014; Gil Montes, 2004; Nogales Basarrarte, 2007; Pizzo, 2004).

In geological terms, the Sierra Bermeja Pluton is located in the southern Iberian Massif (Figure 2) that is at the innermost part of the Variscan Foldbelt characterised by large granitic batholiths (e.g. Bea, Montero, & Zinger, 2003; Castro et al., 2002; Corretgé, Ugidos, & Martínez, 1977; Roda-Robles et al., 2018; Villaseca, Barbero, & Rogers, 1998; Villaseca & Herreros, 2000). Among these batholiths, stand out the cordierite-bearing monzogranites of the so-called 'Serie Mixta' (mixed series), whose origin sits between hybrid (crustal + mantle) and exclusively crustal (e.g. Alonso Olazabal, Carracedo, & Aranguren, 1999; Castro et al., 1999; Castro et al., 2002; Corretgé et al., 1977; Corretgé, Castro, & García-Moreno, 2004; García-Moreno, Corretgé, & Castro, 2007; González Menéndez, 2002). In this sense, the Sierra Bermeja Pluton is suitable for the study of the genesis of these particular granitoids.

At the local scale, the pluton locates in the middle of the Variscan Nisa-Alburquerque-Los Pedroches Magmatic Alignment (Figure 2, Main Map), close to one of the major suture zones of the SW Iberian Massif (e.g. Bandrés et al., 2004; García-Lobón et al., 2014; Martín Parra et al., 2006). In the studied area, two Orogenic Cycles are recognised: the Cadomian Orogeny, better discerned south of the suture zone, and the Variscan Orogeny, the most notorious one north of the

Table 1. Inventory of Geological Points of Interest (GPI).

N° GPI	Coord. (UTM zone 29N)		Description
	X	Y	
GPI-01	731395.7	4325975.4	Neoproterozoic dioritoids
GPI-02	746042.3	4326708.9	Paleozoic shales. slates and quartzites
GPI-03	744905.3	4322601.3	Intrusive contact between monzogranites and host rocks
GPI-04	738039.9	4324331.9	Andalusite spotted hornfels
GPI-05	735972.4	4330687.4	Cenozoic cover
GPI-06	744876.8	4322667.8	Intrusion of MU into the OU (the Rugidero Berrocal)
GPI-07	744593.7	4322852.4	OU main type
GPI-08	744842.8	4322705.8	K-feldspar phenocrysts large accumulations (The Rugidero Berrocal)
GPI-09	741257.0	4329020.7	K-feldspar phenocrysts large accumulations
GPI-10	740853.9	4323779.4	Microgranular mafic magmatic enclaves
GPI-11	745493.0	4325834.1	OU local variety
GPI-12	745190.2	4325997.4	Sheet-by-sheet intrusions between the main type of the OU and its local variety
GPI-13	744208.3	4326525.5	Intrusion of MU into the OU
GPI-14	740363.8	4327180.8	Mixing/mingling relations between the MU and IU
GPI-15	736734.4	4327626.1	Mixing/mingling relations between the MU and IU
GPI-16	740774.4	4324875.0	MU main type
GPI-17	741751.6	4325037.4	MU main type
GPI-18	745440.4	4324367.9	MU local variety
GPI-19	743868.0	4323996.8	MU local variety
GPI-20	738828.1	4327985.1	IU main type
GPI-21	735835.3	4328694.3	IU main type
GPI-22	743934.1	4325161.2	IU local variety
GPI-23	738380.1	4328359.7	Vaugnerite series rocks
GPI-24	737667.2	4327342.9	Vaugnerite series rocks
GPI-25	742424.8	4323984.0	Lamprophyre dyke
GPI-26	743902.8	4324799.1	Lamprophyre dyke
GPI-27	744399.3	4324809.0	Aplite dyke
GPI-28	738511.4	4327835.7	Quartz dyke

suture zone. The Cadomian Cycle corresponds to an episode of Andean-type geodynamic evolution developed between Cryogenian–Early Cambrian, while the Variscan Cycle is a diachronous multi-stage orogeny that resulted ultimately in the assembly of Pangea during the Late Devonian–Early Permian, caused by the collision of Gondwana and Laurentia-Baltica-Avalonia (Eguíluz, Gil Ibarguchi, Ábalos, & Apraiz, 2000; Martínez Catalán et al., 2007). South of the suture zone, the basement is constituted by Late Neoproterozoic–Lower Cambrian metasedimentary and metavolcanic successions (Bandrés et al., 2004; Palacios et al., 2013), known in the regional literature as 'Serie Negra' (black series). On the contrary, in the North is distinctive a Neoproterozoic–Lower Cambrian ensemble of detritic, schistose and greywacke materials (Palacios et al., 2013), termed traditionally as 'Schist-Greywacke Complex' (Figure 2, Main Map). Overlying unconformably the two aforementioned major metasedimetary sequences follows a Paleozoic (Ordovician–Devonian) siliciclastic metasedimentary succession, culminating with the syn-orogenic Culm facies (Palacios et al., 2013). A distinctive feature is the presence of Cadomian igneous intrusive rocks placed south of a crustal scale fault, the so-called 'Alegrete-San Pedro de Mérida-Montoro' thrust (e.g. Bandrés, Eguíluz, Gil Ibarguchi, & Palacios, 2002; Bandrés et al., 2004; Castro, 1988; Figure 2, Main Map). The main Variscan folds consist of NW–SE striking, kilometre-scale upright to slightly south-verging anticlines and synclines, whereas the main Variscan faults correspond to large-scale left-lateral or normal displacement thrusts to the north, roughly parallel to the axial traces of the anticlines and synclines (Bandrés et al., 2004; García-Lobón et al., 2014; Palacios et al., 2013).

3. Previous cartographic works

Published maps that include the Sierra Bermeja Pluton were developed in the frame of regional scale geological projects. For this reason, in these maps the terminology and spatial distribution of granitic units within this pluton are confusing. The first maps (1:50,000 scale) date back to 1946 and 1949 and were conducted by the Geological and Mining Institute of Spain (IGME) during the first MAGNA series (Marín y Bertrán de Lís, 1946; Roso de Luna & Pacheco, 1949). These maps were later updated in a second MAGNA series (Del Olmo Sanz, Matia Villarino, Olivé Davó, & Huerta Carmona, 1992; López Sopena, Matia Villarino, del Olmo, & Ortega Ruiz, 1990). Previously to the second MAGNA series, Gonzalo (1987) proposed a geological scheme for the area of Mérida (1:2,50,000 scale) distinguishing a biotite-bearing porphyritic granite in the outermost sector of the pluton, and a two-mica cordierite-bearing granite in the centre. Afterwards, Sarrionandia, Carracedo, Eguíluz, and Apalategui (2004) proposed another geological scheme (1:2,50,000 scale) of the Sierra Bermeja Pluton dividing the two mica-cordierite bearing granite of Gonzalo (1987) in two new units. Since 2004, the IGME is providing the Continuous Geological map of Spain (GEODE) at 1:50,000 scale but the detailed cartographic information of the Sierra Bermeja Pluton still remains unsolved in that continuous map.

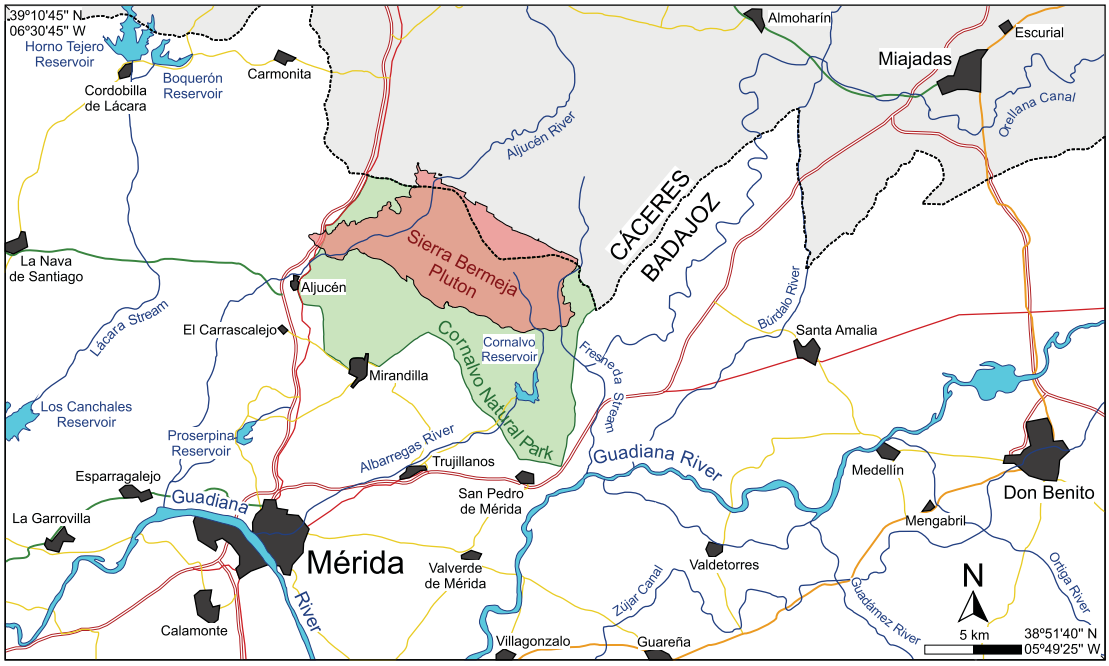

Figure 1. Geographical map showing the location of the Sierra Bermeja Pluton.

4. Methods

Preliminary research was made by means of the interpretation of Light Detection And Ranging (LIDAR) images of 5 m resolution and ortophotographs of the National Plan of Aerial Ortophotography (PNOA, 2009, 2011, 2013). Image analysis allowed the location of the main outcrops, planning of field itineraries and delineation of the contact between granites and host rocks. This preliminary map design was at 1:25,000 scale, using the Mirandilla (0752-IV), Carmonita (0752-II) and Conquista del Guadiana (0753-III) sheets of the Topographic Map of Spain (MTN).

The fieldwork scale was 1:5000, establishing 447 observation stations (7–8 station/km^2) that were georeferenced by a Geographical Positioning System (GPS) receiver. During 42 days of fieldwork the outcrops were described in detail in terms of rock structure, texture,

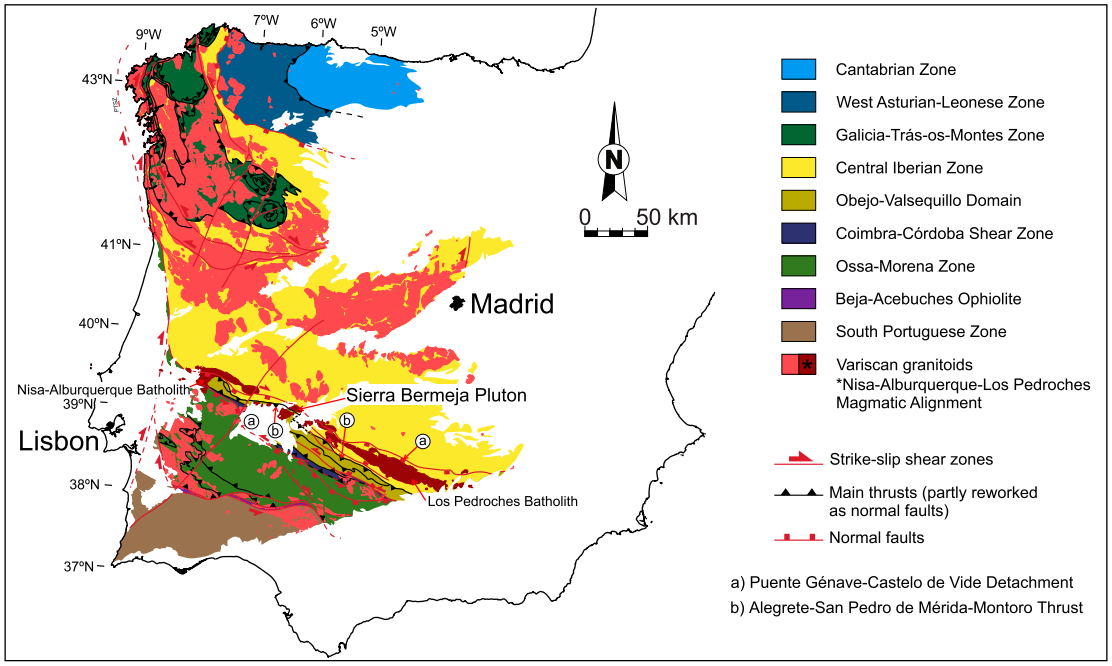

Figure 2. Geological map of the Iberian Massif. The Nisa-Alburquerque-Los Pedroches Magmatic Alignment is emphasised. The subdivision of the Iberian Massif is based on Julivert, Marcos, and Truyols (1972); the extent of the Obejo-Valsequillo domain is based on Bandrés et al. (2004), Martín Parra, González Lodeiro, Martínez Poyatos, and Matas (2006) and Palacios et al. (2013); Variscan granitoids adapted from Rodríguez Fernández and Oliveira (2015); and major tectonic elements adapted from Díez Fernández and Arenas (2015).

fabric and mineralogy. In order to determine the different rock types that constitute this pluton, a series of criteria were defined. Rocks classification in each observation station following these criteria allowed to establish the rock types with a high level of detail in the map. Additionally, detailed field observations allowed to establish the spatial and timing relations between the different rock types. Finally, an inventory of 28 Geological Point of Interest (GPI; Table 1) and 5 sites of interest (Main Map) was generated in order to contribute in the Geological Heritage.

Afterwards, 137 rock-samples (~2 sample/km^2) were collected for complementary petrographic studies in thin section using a polarising microscope Leica DM LP model fitted with a CCD camera in the Mineralogy and Petrology Department of the University of the Basque Country (UPV/EHU). The proportions of monzogranite rock-forming minerals were obtained by point-count modal analyses (Table 2). Finally, for the drawing of the presented map, the cartographic standards for geologic maps (Federal Geographic Data Committee, 2006) were followed, as much as possible.

5. Map description

The Sierra Bermeja Pluton is a 59.75 km^2 elongated trapezoidal-shape intrusion (5.0–7.0 km width; 9.5–12.0 km length), with the long axis oriented N120°E. This massif encompasses several cordierite-bearing monzogranite lithotypes that can be grouped into three main units, which according to their roughly spatial concentric arrangement have been termed as Outer Unit (OU), Middle Unit (MU) and Inner Unit (IU). The contacts between the OU and MU are sharp and curvilinear, whereas those between the MU and IU are complex, resulting on a 100–400 m width belt of heterogeneous monzogranitic masses. This pluton includes also a reduced dyke complex mostly represented by vaugnerite series rocks and calc-alkaline lamprophyres trending NE–SW. The dyke complex of the Sierra Bermeja Pluton includes also minor amounts of aplite and quartz dykes.

The Sierra Bermeja Pluton intrudes into Neoproterozoic dioritoids (GPI-01; Bandrés et al., 2004) and a Paleozoic (Ordovician–Carboniferous) metasedimentary sequence constituted by shales, slates and quartzites (GPI-02; Palacios et al., 2013). This sequence exhibits N120–140E strike and a low-grade regional metamorphism. The intrusive contacts with the host rocks are sharp (GPI-03), but only visible in the North and South edges of the pluton where some faults have been inferred. The intrusion generated a contact metamorphism aureole in the Paleozoic sequence constituted by andalusite spotted hornfels in a 400–600 m width band (GPI-04), whereas in the Neoproterozoic dioritoids there are no apparent effects. By contrast, in the East and West areas the cordierite-bearing monzogranites are hidden under thick alluvial and colluvial deposits (Cenozoic cover; GPI-05).

6. Cordierite-bearing monzogranites of the Sierra Bermeja Pluton

6.1. Outer Unit (OU)

This unit extends along the outermost areas of the pluton, subparallel to the northern and southern limits of the massif in three separated sectors encompassing 20.03 km^2 (33.5% of the total area of the pluton; t.a.p.). Outward, it limits with the host rocks showing sharp intrusive contacts (Figure 3(a)) that appear segmented by decametre-scale displacements (up to 250 m) along N-NE trending faults, and inward with the MU. The temporal emplacement relation between both units is deducible in several areas of the pluton, standing out the outcrop of the Rugidero Berrocal (GPI-06), where a dyke of the MU intrudes the OU (Figure 3(b); Main Map).

The OU is constituted by white monzogranites that show a massive or homophanous structure and a planar/linear fabric. This fabric is defined by fairly oriented (N100–170E, subhorizontal) K-feldspar phenocrysts that can reach up to 12 cm in length. The concentration of these phenocrysts is markedly high (150–350 crystals/m^2; 10–35% vol.), which confers a porphyritic texture to these rocks and constitutes the most characteristic feature of this unit (Figure 3(c); GPI-07). The phenocrysts are included in a holocrystalline phaneritic (medium- to coarse-grained) biotite-rich granodioritic groundmass, constituted by euhedral plagioclase (up to 15 mm), globular quartz (up to 11 mm), K-feldspar (up to 10 mm), biotite (up to 3 mm) and cordierite (up to 6 mm). Besides the K-feldspar phenocrysts, at the outcrop scale this unit is also characterised by the relative abundance of globular quartz and biotite, and the relative scarcity of cordierite as compared to the other units (Table 2). Larger accumulations of phenocrysts (up to 750 crystals/m^2; GPI-08; GPI-09), tonalitic microgranular mafic magmatic enclaves (Figure 3(d); GPI-10), rare felsic-microgranular enclaves and pelitic xenoliths, and biotite schlieren are found sparsely in the OU. Also, in several outcrops pegmatite, aplite and aplopegmatite veins are observed, all of them on the order of centimetres in width.

Within the OU stands out a fine-grained variety characterised by a greater abundance of biotite, and lower amounts of cordierite and globular quartz (Table 2; GPI-11). The size of the K-feldspar phenocrysts is also smaller in this variety (up to 6 cm long) that crops out in three small irregular masses representing 4.8% of the OU surface area (0.97 km^2). These masses are located in the eastern sector of the pluton in contact with the medium- to coarse-grained

Table 2. Key features of monzogranite types of the Sierra Bermeja Pluton.

	Outer Unit (OU)		Middle Unit (MU)		Inner Unit (IU)	
	Main type	Local variety	Main type	Local variety	Main type	Local variety
Enclaves	Mafic and felsic magmatic; pelitic	Mafic and felsic magmatic; pelitic	–	–	–	–
Kfs phenocrysts	150–350/m^2	150–250/m^2	Occasional	Occasional	–	–
Groundmass crystal-syze	Medium to coarse	Fine to medium	Medium to coarse	Medium to coarse	Fine to medium	Fine to medium
Quartz	27–35%	26–38%	31–40%	33–39%	32–41%	31–38%
Kfs (groundmass)	15–28%	14–27%	24–33%	25–32%	22–30%	24–31%
Plagioclase	33–42%	34–45%	26–35%	25–33%	24–32%	25–32%
Cordierite	1–5%	1–3%	5–10%	1–5%	2–7%	1–3%
Biotite	6–11%	9–14%	3–6%	5–7%	1–4%	3–7%
Muscovite	0–1%	0–1%	0–2%	0–2%	2–8%	2–4%
Accessory minerals	Ap, Mnz, Zrn, Xtm, Tur, Ilm	Ap, Mnz, Zrn, Xtm, Tur, Ilm	Ap, Mnz, Zrn, Xtm, Tur, Ilm	Ap, Mnz, Zrn, Xtm, Tur, Ilm	Ap, Mnz, Zrn, Xtm, Tur, And, Ilm, Rt	Ap, Mnz, Zrn, Xtm, Tur, And, Ilm, Rt

monzogranites of the OU, the host rocks and the MU (Main Map). The timing relation between this local variety and the medium- to coarse-grained monzogranites of the OU is deducible from the observed sheet-by-sheet intrusion relationships (GPI-12) that indicate their coetaneous emplacement.

6.2. Middle Unit (MU)

This unit is located between the aforementioned OU and the IU covering a surface area of 24.49 km^2 (41.0% t.a.p.). The external limits of this unit are sharp and curvilinear, which may be regarded as a consequence of its intrusion into the host rocks and the monzogranites of the OU (GPI-13). On the contrary, the relation with the IU is defined by a 100–400 m width heterogeneous belt that covers an area of 5.38 km^2 (9.0% t.a.p.; Main Map). This belt is constituted by rocks with intermediate characteristics between those of the MU and IU, besides the sheet-by-sheet intrusion zones between both units (GPI-14; GPI-15). This evidences that mixing and mingling processes occurred between the MU and IU.

The MU is constituted by apparently undeformed white monzogranites showing a massive or homophanous structure. Only in some outcrops a planar/linear fabric is observable related to local metre-scale shear zones. These rocks exhibit a medium- to coarse-grained hypidiomorphic seriated texture and are constituted by globular quartz (up to 19 mm), plagioclase (up to 15 mm), K-feldspar (up to 16 mm), euhedral cordierite (up to 18 mm) and biotite (up to 2 mm). K-feldspar phenocrysts (up to 6 cm) are scarce (<5 crystals/m^2) and are usually found close to the OU–MU contact. The monzogranites of this unit differ from those of the OU because of their drastic lower K-feldspar phenocryst and markedly higher cordierite contents (Figure 3(e); GPI-16: GPI-17). Besides that, biotite amounts are lower in the MU (Table 2). Small accumulations of K-feldspar phenocrysts (20–50 crystals), as well as rare pegmatite, aplite and aplopegmatite veins/segregates are observed in this unit too.

Locally within the MU a subtype of monzogranite can be discerned (GPI-18; GPI-19). It crops out in two distinct areas of the pluton (Main Map) covering a surface of 5.66 km^2 (23.1% of the MU). This variety is distinguished from the main type by the greater abundance of biotite and markedly lower cordierite content (Table 2). The relation between both monzogranites of the MU is controversial. Nevertheless, the observed variations in texture within this subtype, close to the main monzogranite type, points to their coeval emplacement.

6.3. Inner Unit (IU)

This unit extends along the pluton axis covering a surface area of 9.38 km^2 (15.7% t.a.p.). It appears dismembered in eight heterometric masses, standing out a ~5 km long and ~2 km width mass located in the westernmost zone of the pluton (Main Map). All these masses are enclosed by the mixing/mingling belt that separates the IU and MU.

The IU is constituted by yellowish monzogranites with massive or homophanous structure and isotropic fabric that, in the westernmost areas, exhibit a well-developed N40–60E trending joint system (GPI-20; GPI-21). Their texture is fine- to medium-grained hypidiomorphic seriated, with low colour index (generally <5) that allows to consider them as leucogranites (Figure 3(f)). Their main mineralogy consists of globular quartz (up to 10 mm), plagioclase (up to 9 mm), K-feldspar (up to 8 mm), muscovite (up to 3 mm), euhedral cordierite (up to 9 mm) and biotite (up to 2 mm). The distinctive features of this unit are the fine crystal-size and the relatively high content of muscovite (Table 2). As in the other monzogranite units, K-feldspar phenocryst clusters (20–50 crystals) and pegmatite, aplite and aplopegmatite veins/segregates are observable (Figure 3(g)).

In the easternmost masses, the cordierite content decreases markedly whereas that of biotite increases (Table 2; GPI-22), which allows to differentiate a local variety within the IU (0.34 km^2; 3.6% of IU). Moreover, the mixing/mingling belt around this variety

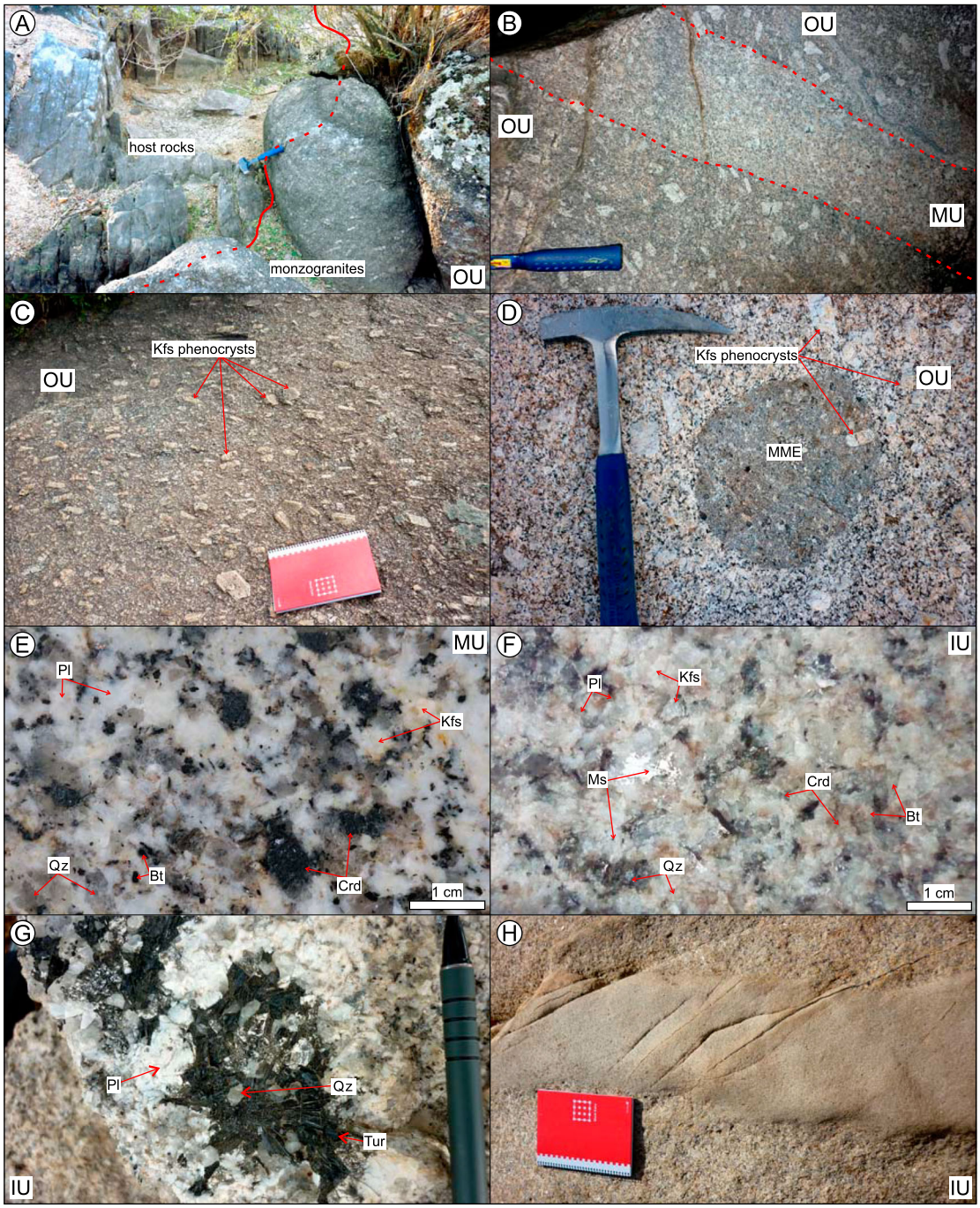

Figure 3. (A) Sharp intrusive contact between the OU monzogranites and host rocks (GPI-03). (B) Dyke of MU intruding into the OU (GPI-06). (C) Moderately oriented Kfs phenocrysts in the OU main monzogranite type (GPI-07). (D) Mafic magmatic enclave including a K-feldspar phenocryst (GPI-10). (E) Scanned section of the MU main monzogranite type. (F) A detail picture of the IU main monzogranite type. (G) Tourmaline in pegmatite segregates. (H) Aplite dyke intruding into the IU.

contacts only with the monzogranite subtype of the MU (Main Map).

7. Vaugnerite series rocks and lamprophyres of the Sierra Bermeja Pluton

7.1. Vaugnerite series rocks

These rocks are restricted to a 4 km long and up to 150 m width, N30–45E trending linear belt. It covers a 0.13 km^2 (0.2% t.a.p.) surface area in the middle-western sector of the pluton (Main Map). At the outcrop scale, this belt is defined by sinuous alignments of decimetre in size, rounded, dark-coloured rock blocks. These blocks do not constitute continuous masses and show variable spacing between them (0.5–3 m) that increases progressively towards the tips of each alignment, up to finally disappear (GPI-23; GPI-24). The timing relation with the host monzogranites is deducible at the cartographic scale with vaugneritic alignments cross-cutting the contacts between the monzogranite units (Main Map). Yet, their sinuous trends, the absence of chilled margins, the necking of the alignments and their dismembered

terminations suggest that they would correspond to syn-plutonic dykes.

These mesocratic rocks show a massive or homophanous structure and present a medium-grained, hypidio-idiomorphic, inequigranular seriated texture. Their main mineralogy includes variable amounts of plagioclase, amphibole, clinopyroxene, biotite, K-feldspar, and quartz. In detail, these mesocratic rocks can be subdivided in two subtypes, which, depending on the modal composition, are here termed as 'biotite-rich' and 'biotite-poor'. Following the IUGS recommendations (Le Maitre et al., 2002) these rocks are classified as diorites, quartz diorites and quartz monzodiorites, but on account of their mineralogy and whole-rock geochemical composition are considered as a whole within the vaugnerite series rocks (see Errandonea-Martin, Sarrionandia, Carracedo-Sánchez, Gil Ibarguchi, & Eguíluz, 2018).

7.2. Lamprophyres

These rocks appear distributed throughout the whole pluton covering a 0.11 km^2 surface area (0.2% t.a.p.). At the outcrop and map scale lamprophyres exhibit characteristics fairly similar to those of vaugnerite series rocks above described. Nevertheless, they usually constitute straight and narrow (<5 m) alignments with NE–SW trends (Main Map). Host monzogranite enclaves are found in some lamprophyres, suggesting the late- to post-intrusive character of these dykes respect to the monzogranites.

These rocks are constituted by homophanous aphanitic mesocratic rocks with porphyritic texture (GPI-25; GPI-26). They are characterised by the presence of clinopyroxene phenocrysts (up to 2 mm), occasionally accompanied by biotite (up to 2 mm) and amphibole (up to 2 mm), included in a microcrystalline groundmass. This aphanitic groundmass is constituted mainly by the same mineralogy as the phenocrysts plus plagioclase (see Errandonea-Martin et al., 2018).

8. Aplites and quartz dykes of the Sierra Bermeja Pluton

Mappable aplites in the Sierra Bermeja Pluton occur as dykes or irregular masses covering 0.14 km^2 (0.2% t.a.p.). Aplite dykes show metre-scale widths and up to 600 m lengths (GPI-27). They present roughly NE–SW trends intruding into the three main monzogranitic units. Mapped aplite masses crop out in the northwestern area of the pluton and intrude both the OU and the host rocks (Main Map). In this massif, aplites -fine-grained leucogranites - are apparently homophanous, and they show a hypidiomorphic seriated texture (Figure 3(h)). Their mineralogy comprises quartz (up to 4 mm), K-feldspar (up to 5 mm), plagioclase (up to 5 mm), muscovite (up to 2 mm) and tourmaline (up to 3 mm).

Quartz dykes form marked positive linear prominences up to 450 m long and 50 m width (Main Map; GPI-28). They show straight N35–45E trends and are constituted by white (locally reddish) quartz crystal aggregates. The host monzoganite close to these dykes shows pervasive hydrothermal alteration.

9. Conclusions

The detailed geologic map of the Sierra Bermeja Pluton presented in this contribution has revealed a complex intrusive assemblage. Three main monzogranite types (showing local varieties) plus a reduced dyke complex composed by vaugnerite series rocks, lamprophyres, aplites and quartz dykes constitute this Variscan massif. Besides, mingling/mixing areas have been mapped for the first time in this type of cordierite-bearing monzogranites of the Iberian Massif. Field relationships indicate that (1) monzogranite pulses are younger towards the centre of the pluton, (2) vaugnerite series rocks form syn-plutonic dykes, and (3) lamprophyres, aplites and quartz dykes intruded after almost the complete consolidation of monzogranites. These outcomes will constitute the basis for forthcoming contributions related to the genesis of these controversial monzogranites.

Additionally, exhaustive fieldwork has allowed to summarise an inventory of relevant sites that comprise several Geologic Points of Interest (GPI), most of them located in the Cornalvo Natural Park. These points of interest, together with the new geologic map produced of the Sierra Bermeja Pluton, should be considered by the relevant institutions in terms of geoconservation and geological heritage. It is hoped that the map will constitute a robust tool in the diffusion and educational objectives for the Cornalvo Natural Park Interpretation Centre.

Software

Garmin Basecamp 4.7.0 was used for: (1) create tracks for the fieldwork, and (2) manage georeferenced points. Esri ArcGIS 10.3 was used for: (1) gathering and visualisation of underlying data, (2) construction of high-resolution digital terrain models, (3) management of field data, (4) digitisation and editing of geologic data layers, and (5) production of the map layout.

Acknowledgements

The authors thank the General Cartography and Geographic Information Systems Service-SGIker (UPV/EHU) and J. Errandonea-Martin also thanks the grant from the UPV/EHU 2014 programme. The authors would like to thank also the review made by Rubén Díez Fernández, Chris

Orton and Stefano Cuccuru and the editorial handling of Mike J. Smith that improve considerably the manuscript and the main map.

Disclosure statement

No potential conflict of interest was reported by the authors.

Funding

The authors thank the financial support of the Spanish Ministerio de Economía y Competitividad Ciencia e Innovación (MINECO, grant CGL2015-63530-P) and the University of the Basque Country (UPV/EHU, Grupo Consolidado project GIU15/05).

ORCID

Jon Errandonea-Martin http://orcid.org/0000-0003-2561-8213

References

Agencia Estatal de Meteorología de España, AEMET. (2012). Guía resumida del clima en España (1981–2010). Retrieved from http://www.aemet.es/es/conocermas/recursos_en_linea/publicaciones_y_estudios/publicaciones/detalles/guia_resumida_2010

Agencia Estatal de Meteorología de España, AEMET & Instituto de Meteorologia de Portugal, IPMA. (2011). *Iberian climate atlas*. Madrid: Closas-Orcoyen.

Alonso Olazabal, A., Carracedo, M., & Aranguren, A. (1999). Petrology, magnetic fabric and emplacement in a strike-slip regime of a zoned peraluminous granite: The Campanario-La Haba pluton, Spain. *Special Publications of the Geological Society of London*, *168*, 177–190. doi:10.1144/GSL.SP.1999.168.01.12

Álvarez Martínez, J. M., & Nogales Basarrarte, T. (2014). Presas de Augusta Emerita y de sus alrededores. In F. Baratte, C. J. Robin, & E. Rocca, (Eds.), *Regards croisés d'Orient et d'Occident. Les barrages dans l'Antiquité tardivet. Actes du colloque organisé dans le cadre du programme ANR EauMaghreb* (pp. 163–177). Paris: Editions De Boccard.

Bandrés, A., Eguíluz, L., Gil Ibarguchi, J. I., & Palacios, T. (2002). Geodynamic evolution of a Cadomian arc region: The northern Ossa-Morena zone, Iberian massif. *Tectonophysics*, *352*(1–2), 105–120. doi:10.1016/S0040-1951(02)00191-9

Bandrés, A., Eguíluz, L., Pin, C., Paquette, J. L., Ordoñez, B., Le Fèvre, B., … Gil Ibarguchi, J. I. (2004). The northern Ossa-Morena Cadomian batholith (Iberian Massif): magmatic arc origin and early evolution. *International Journal of Earth Sciences*, *93*(5), 860–885. doi:10.1007/s00531-004-0423-6

Barral I Altet, X. (1991). La Antigüedad Clásica: Grecia, Roma y El Mundo Mediterraneo. In J. Milicua (Ed.), *Historia Universal del Arte* (Vol. 2, p. 391). Vitoria: Planeta.

Bea, F., Montero, P., & Zinger, T. (2003). The nature, origin, and thermal influence of the granite source layer of central Iberia. *The Journal of Geology*, *111*, 579–595. doi:10.1086/376767

Bonin, B., Azzouni-Sekkal, A., Bussy, F., & Ferrag, S. (1998). Alkali-calcic and alkaline post-orogenic (PO) granite magmatism: Petrologic constraints and geodynamic settings. *Lithos*, *45*, 45–70. doi:10.1016/S0024-4937(98)00025-5

Brilha, J. (2002). Geoconservation and protected areas. *Environmental Conservation*, *29*(3), 273–276. doi:10.1017/S0376892902000188

Brocx, M., & Semeniuk, V. (2007). Geoheritage and geoconservation - history, definition, scope and scale. *Journal of the Royal Society of Western Australia*, *90*, 53–87.

Carreras, J., & Druguet, E. (2000). Geological heritage, an essential part of the integral management of world heritage in protected sites. In D. Barettino, W. A. P. Wimbledon, & E. Gallego (Eds.), *Geological heritage: Its conservation and management. III International Symposium ProGEO on the conservation of the geological heritage* (pp. 95–110). Madrid: Instituto Tecnológico Geominero de España.

Casini, L., Cuccuru, S., Maino, M., Oggiano, G., Puccini, A., & Rossi, P. (2015). Structural map of Variscan northern Sardinia (Italy). *Journal of Maps*, *11*(1), 75–84. doi:10.1080/17445647.2014.936914

Castro, A. (1988). Los granitoides deformados de la banda del Guadámez (La Serena, Badajoz). In F. Bea, A. Carnicero, J. C. Gonzalo, M. López Plaza, & M. D. Rodríguez Alonso (Eds.), *Geologia de los granitoides y rocas asociadas del Macizo Hespérico: Libro homenaje a L.C. García Figuerola* (pp. 413–426). Madrid: Rueda.

Castro, A., Corretgé, L. G., De la Rosa, J., Enrique, P., Martínez, F. J., Pascual, E., … López, S. (2002). Paleozoic Magmatism. In W. Gibbons, & T. Moreno (Eds.), *The geology of Spain* (pp. 117–153). London: Geological Society.

Castro, A., Patiño-Douce, A., Corretgé, L. G., De la Rosa, J., El-Biad, M., & El-Hmidi, H. (1999). Origin of peraluminous granites and granodiorites, Iberian Massif, Spain: An experimental test of granite petrogenesis. *Contributions to Mineralogy and Petrology*, *135*(2), 255–276. doi:10.1007/s004100050511

Chakhmouradian, A. R., & Zaitsev, A. N. (2012). Rare Earth Mineralization in igneous rocks: Sources and processes. *Elements*, *8*(5), 347–353. doi:10.2113/gselements.8.5.347

Cobbing, J. (2000). *The geology and mapping of granite batholiths*. Berlin Heidelberg: Springer-Verlag. doi:10.1007/3-540-45055-6

Corretgé, L. G., Castro, A., & García-Moreno, O. (2004). Granitoides de la 'serie mixta'. In J. A. Vera (Ed.), *Geología de España* (pp. 115–116). Madrid: Sociedad Geológica de España e Instituto Geológico y Minero de España.

Corretgé, L. G., Ugidos, J. M., & Martínez, F. J. (1977). Les series granitiques varisques du secteur centre-Occidental Espagnol. La chaine varisque d'Europe moyenne et occidentale. *Colloque International du Centre National de la Recherche Scientffique*, *243*, 453–461.

Del Olmo Sanz, A., Matia Villarino, G., Olivé Davó, A., & Huerta Carmona, J. (1992). Hoja geológica número 752 (Mirandilla). *Mapa Geológico de España a Escala 1:50.000 (2ª serie)*. Madrid: Instituto Geológico y Minero de España (IGME). Retrived from http://info.igme.es/cartografiadigital/geologica/Magna50Hoja.aspx?Id=752

Dingwall, P. R. (2000). Legislation and International Agreements: The integration of the geological heritage in nature conservation policies. In D. Barettino, W. A. P. Wimbledon, & E. Gallego (Eds.), *Geological heritage: Its conservation and management. III International Symposium ProGEO on the conservation of the geological heritage* (pp. 15–28). Madrid: Instituto Tecnológico Geominero de España.

Díez Fernández, R., & Arenas, R. (2015). The late devonian Variscan suture of the Iberian massif: a correlation of high-pressure belts in NW and SW Iberia. *Tectonophysics*, *654*, 96–100. doi:10.1016/j.tecto.2015.05.001

Díez Fernández, R., Martín Parra, L. M., & Rubio Pascual, F. J. (2017). Extensional flow produces recumbent folds in syn-orogenic granitoids (Padrón migmatitic dome, NW Iberian Massif). *Tectonophysics*, *703–704*, 69–84. doi:10.1016/j.tecto.2017.03.010

Díez Fernández, R., Rubio Pascual, F. J., & Martín Parra, L. M. (2018). Re-folded structure of syn-orogenic granitoids (Padrón dome, NW Iberia): assessing rheological evolution of cooling continental crust in a collisional setting. *Geoscience Frontiers*. In Press. doi:10.1016/j.gsf.2018.03.007

Eguíluz, L., Gil Ibarguchi, J. I., Ábalos, B., & Apraiz, A. (2000). Superposed Hercynian and Cadomian orogenic cycles in the Ossa-Morena zone and related areas of the Iberian Massif. *Geological Society of America Bulletin*, 1398–1413. https://doi.org/10.1130/0016-7606(2000)112<1398:SHACOC>2.0.CO;2

Errandonea-Martin, J., Sarrionandia, F., Carracedo-Sánchez, M., Gil Ibarguchi, J. I., & Eguíluz, L. (2018). Petrography and geochemistry of late- to post-Variscan vaugnerite series rocks and calc-alkaline lamprophyres within a cordierite-bearing monzogranite (the Sierra Bermeja Pluton, southern Iberian Massif). *Geologica Acta*, *16*(3), 237–255. doi:10.1344/GeologicaActa2018.16.3.1

Federal Geographic Data Committee [prepared for the Federal Geographic Data Committee by the U.S. Geological Survey]. (2006). FGDC Digital Cartographic Standard for Geologic Map Symbolization: Reston, Va., Federal Geographic Data Committee Document Number FGDC-STD-013-2006, p. 290 , 2 plates.

García-Lobón, J. L., Rey-Moral, C., Ayala, C., Martín-Parra, L. M., Matas, J., & Reguera, M. I. (2014). Regional structure of the southern segment of Central Iberian zone (Spanish Variscan Belt) interpreted from potential field images and 2.5 D modelling of Alcudia gravity transect. *Tectonophysics*, *614*, 185–202. doi:10.1016/j.tecto.2013.12.005

García-Moreno, O., Corretgé, L. G., & Castro, A. (2007). Processes of assimilation in the genesis of cordierite leucomonzogranites from the Iberian massif: A short review. *The Canadian Mineralogist*, *45*, 71–85. doi:10.2113/gscanmin.45.1.71

Gil Montes, J. (2004). Via delapidata. Identificación de una carretera romana por la procedencia de los materiales. In Colegio de Ingenieros Técnicos de Obras Públicas (Ed.), *Elementos de ingeniería romana. Congreso europeo* '*Las obras públicas romanas*' (pp. 87–102). Tarragona: Colegio de Ingenieros Técnicos de Obras Públicas.

González Menéndez, L. (2002). Petrología del Batolito Granítico de Nisa-Alburquerque. *Revista de la Sociedad Geológica de España*, *15*(3–4), 233–246.

Gonzalo, J. C. (1987). *Petrología y estructura del basamento hercínico del área de Mérida (Extremadura Central)* (*Doctoral dissertation*). University of Salamanca, Salamanca.

Hawkesworth, C. J., Dhuime, B., Pietranik, A. B., Cawood, P. A., Kemp, A. I. S., & Storey, C. D. (2010). The generation and evolution of the continental crust. *Journal of the Geological Society*, *167*, 229–248. doi:10.1144/0016-76492009-072

Julivert, M., Marcos, A., & Truyols, J. (1972). L'évolution paléogéographique du NW de l'Espagne pendant l'Ordovicien-Silurien. *Bulletin de la Société Géologique et minéralogique de Bretagne*, *4*, 1–7.

Le Maitre, R. W., Streckeisen, A., Zanettin, B., Le Bas, M. J., Bonin, B., Bateman, P., … Woolley, A. R. (2002). *Igneous rocks: A classification and glossary of terms*. Cambridge: Cambridge University Press. doi:10.2113/gscanmin.40.6.1737

Linnen, R. L., Lichtervelde, M. V., & Černý, P. (2012). Granitic pegmatites as sources of strategic metals. *Elements*, *8*(4), 275–280. doi:10.2113/gselements.8.4.275

Lisle, R. J., Brabham, P., & Barnes, J. (2011). *Basic geological mapping* (5th ed.). Chichester: Wiley-Blackwell.

López Sopena, F., Matia Villarino, G., del Olmo, A., & Ortega Ruiz, I. (1990). Hoja geológica número 753 (Miajadas). *Mapa Geológico de España a Escala 1:50.000* (2ª serie). Madrid: Instituto Geológico y Minero de España (IGME). Retrieved from http://info.igme.es/cartografiadigital/geologica/Magna50Hoja.aspx?id=753

Marín y Bertrán de Lís, A. (1946). Hoja geológica número 753 (Miajadas). Mapa Geológico de España a Escala 1:50.000 (1ª serie). Madrid: Instituto Geológico y Minero de España (IGME). Retrieved from http://info.igme.es/cartografiadigital/geologica/Geo50Hoja.aspx?Id=753&language=es

Martínez Catalán, J. R., Arenas, R., Díaz García, F., Gómez-Barreiro, J., González-Cuadra, P., Abati, J., … Valle Aguado, B. (2007). Space and time in the tectonic evolution of the northwestern Iberian Massif. Implications for the comprehension of the Variscan belt. In R. D. Hatcher, M. P. Carlson, J. H. Mcbride, & J. R. Martínez Catalán (Eds.), *4-D framework of continental crust* (p. 200). Boulder, CO: Geological Society of America Memoir.

Martín Parra, L. M., González Lodeiro, F., Martínez Poyatos, D., & Matas, J. (2006). The Puente Génave-Castelo de Vide shear zone (Southern Central Iberian Zone, Iberian Massif): Geometry, kinematics and regional implications. *Bulletin de la Société Géologique de France*, *177*(4), 191–202. doi:10.2113/gssgfbull.177.4.191

Nogales Basarrarte, T. (2007). Teatro romano de Augusta Emerita. Evolución y programas decorativos. *Mainake*, *29*, 103–138.

Palacios, T., Eguíluz, L., Apalategui, O., Jensen, S., Martínez-Torres, L. M., Carracedo, M., … Martí, M. (2013). *Mapa Geológico de Extremadura 1/350.000 y su memoria*. Bilbao: Servicio Editorial de la UPV-EHU. 68×98 cm, p. 222.

Pitcher, W. S. (1997). *The nature and origin of granite* (2nd ed.). Dordrecht: Springer. doi:10.1007/978-94-011-5832-9

Pizzo, A. (2001). La casa del Anfiteatro de Augusta Emerita. *Mérida, excavaciones arqueológicas*, *7*, 335–350.

Porquet, M., Pueyo, E. L., Román-Berdiel, T., Olivier, P., Longares, L. A., Cuevas, J., … Vegas, N. (2017). Anisotropy of magnetic susceptibility of the Pyrenean granites. *Journal of Maps*, *13*(2), 438–448. doi:10.1080/17445647.2017.1302364

Roda-Robles, E., Villaseca, C., Pesquera, A., Gil-Crespo, P. P., Vieira, R., Lima, A., & Garate-Olave, I. (2018). Petrogenetic relationships between Variscan granitoids and Li-(F-P)-rich aplite-pegmatites in the Central Iberian zone: Geological and geochemical constraints and implications for other regions from the European Variscides. *Ore Geology Reviews*, *95*, 408–430. doi:10.1016/j.oregeorev.2018.02.027

Rodríguez Fernández, L. R., & Oliveira, J. T. (2015). Mapa geológico de España y Portugal a escala 1:1.000.000. *Instituto Geológico y Minero de España, Laboratório*

Nacional de Energia e Geologia de Portugal. Retreived from http://info.igme.es/cartografiadigital/geologica/GeologicosMMapa.aspx?Id=Geologico1000_(2015)

Roso de Luna, I., & Pacheco, F. H. (1949). Hoja geológica número 752 (Mirandilla). *Mapa Geológico de España a Escala 1:50.000 (1ª serie)*. Madrid: Instituto Geológico y Minero de España (IGME). Retrieved from http://info.igme.es/cartografiadigital/geologica/Geo50Hoja.aspx?Id=752&language=es

Rudnick, R. L., & Gao, S. (2014). Composition of the continental crust. *Treatise on Geochemistry*, *4*, 1–51. doi:10.1016/B978-0-08-095975-7.00301-6

Sarrionandia, F., Carracedo, M., Eguíluz, L., & Apalategui, O. (2004). Potencial ornamental del plutón de Sierra Bermeja (Badajoz): Evaluación de su canterabilidad. *Geogaceta*, *35*, 103–106.

Sarrionandia, F., Carracedo, M., Eguíluz, L., Junguitu, J., Lobo, P., & Gil Ibarguchi, J. I. (2013). Geologic map of the Valencia del Ventoso Variscan igneous complex (SW Iberian Massif, Spain): An example of multi-stage intrusion building by contrasted magma compositions. *Journal of Maps*, *9*(4), 498–504. doi:10.1080/17445647.2013.820675

Sial, A. N., Bettencourt, J. S., De Campos, C. P., & Ferreira, V. P. (2011). Granite-related ore deposits: An introduction. *Geological Society of London, Special Publications*, *350*, 1–5. doi:10.1144/SP350.1

Sureda, J. (1991). Las Primeras Civilizaciones: Prehistoria. Egipto. Próximo Oriente. In J. Milicua (Ed.), *Historia Universal del Arte* (Vol. 1, p. 401). Vitoria: Planeta.

Villaseca, C., Barbero, L., & Rogers, G. (1998). Crustal origin of Hercynian peraluminous granitic batholiths of Central Spain: Petrological, geochemical and isotopic (Sr, Nd) constraints. *Lithos*, *43*(2), 55–79. doi:10.1016/S0024-4937(98)00002-4

Villaseca, C., & Herreros, V. (2000). A sustained felsic magmatic system: The Hercynian granitic batholith of the Spanish central system. *Earth and Environmental Science Transactions of the Royal Society of Edinburgh*, *91*, 207–219. doi:10.1017/S0263593300007380

Wilson Jones, M. (2000). *Principles of roman architecture*. Singapore: Yale University Press.

Wimbledon, W. A. P., Ishchenko, A. A., Gerasimenko, N. P., Karis, L. O., Suominen, V., Johansson, C. E., & Freden, C. (2000). Geosites - an IUGS initiative: Science supported by conservation. In D. Barettino, W. A. P. Wimbledon, & E. Gallego (Eds.), *Geological heritage: Its conservation and management. III International Symposium ProGEO on the conservation of the geological heritage* (pp. 69–94). Madrid: Instituto Tecnológico Geominero de España.